

## Spatial and temporal variability in summertime dissolved carbon dioxide and methane in temperate ponds and shallow lakes

Nicholas E. Ray  <sup>1\*</sup>, Meredith A. Holgerson  <sup>1</sup>, Mikkel Rene Andersen <sup>2</sup>, Jānis Bikše <sup>3</sup>, Lauren E. Bortolotti  <sup>4</sup>, Martyn Futter <sup>5</sup>, Ilga Kokorīte <sup>6</sup>, Alan Law  <sup>7</sup>, Cory McDonald  <sup>8</sup>, Jorrit P. Mesman <sup>9,10</sup>, Mike Peacock  <sup>5,11</sup>, David C. Richardson <sup>12</sup>, Julien Arsenault  <sup>13</sup>, Sheel Bansal <sup>14</sup>, Kaelin Cawley <sup>15</sup>, McKenzie Kuhn <sup>16</sup>, Amir Reza Shahabinia <sup>17</sup>, Facundo Smufer  <sup>17</sup>

<sup>1</sup>Department of Ecology and Evolutionary Biology, Cornell University, Ithaca, New York, USA

<sup>2</sup>Centre for Freshwater and Environmental Studies, Dundalk Institute of Technology, Dundalk, Ireland

<sup>3</sup>Faculty of Geography and Earth Sciences, University of Latvia, Riga, Latvia

<sup>4</sup>Institute for Wetland and Waterfowl Research, Ducks Unlimited Canada, Stonewall, Manitoba, Canada

<sup>5</sup>Department of Aquatic Sciences and Assessment, Swedish University of Agricultural Sciences, Uppsala, Sweden

<sup>6</sup>Institute of Biology, University of Latvia, Riga, Latvia

<sup>7</sup>Biological and Environmental Sciences, University of Stirling, Stirling, UK

<sup>8</sup>Department of Civil, Environmental, and Geospatial Engineering, Michigan Technological University, Houghton, Michigan, USA

<sup>9</sup>Department of Ecology and Genetics, Uppsala University, Uppsala, Sweden

<sup>10</sup>Department F.A. Forel for Environmental and Aquatic Sciences, University of Geneva, Geneva, Switzerland

<sup>11</sup>Department of Geography and Planning, School of Environmental Sciences, University of Liverpool, Liverpool, UK

<sup>12</sup>Biology Department, State University of New York at New Paltz, New Paltz, New York, USA

<sup>13</sup>Groupe de Recherche Interuniversitaire en Limnologie (GRIL), Département de Géographie, Université de Montréal, Montréal, Québec, Canada

<sup>14</sup>U.S. Geological Survey, Northern Prairie Wildlife Research Center, Jamestown, North Dakota, USA

<sup>15</sup>Battelle, NEON Project, Boulder, Colorado, USA

<sup>16</sup>Department of Earth Sciences and Earth System Research Center, Institute for the Study of Earth, Ocean and Space, University of New Hampshire, Durham, New Hampshire, USA

<sup>17</sup>Groupe de Recherche Interuniversitaire en Limnologie (GRIL), Département des Sciences Biologiques, Université du Québec à Montréal, Montréal, Québec, Canada

### Abstract

Small waterbodies have potentially high greenhouse gas emissions relative to their small footprint on the landscape, although there is high uncertainty in model estimates. Scaling their carbon dioxide ( $\text{CO}_2$ ) and methane ( $\text{CH}_4$ ) exchange with the atmosphere remains challenging due to an incomplete understanding and characterization of spatial and temporal variability in  $\text{CO}_2$  and  $\text{CH}_4$ . Here, we measured partial pressures of  $\text{CO}_2$  ( $p\text{CO}_2$ ) and  $\text{CH}_4$  ( $p\text{CH}_4$ ) across 30 ponds and shallow lakes during summer in temperate regions of Europe and North America. We sampled each waterbody in three locations at three times during the growing season, and tested which physical, chemical, and biological characteristics related to the means and variability of  $p\text{CO}_2$  and  $p\text{CH}_4$  in space and time. Summer means of  $p\text{CO}_2$  and  $p\text{CH}_4$  were inversely related to waterbody size and positively related to floating vegetative cover;  $p\text{CO}_2$  was also positively related to dissolved phosphorus. Temporal variability in partial pressure in both gases was greater than spatial variability. Although sampling on a single date was likely to misestimate mean seasonal  $p\text{CO}_2$  by up to 26%, mean seasonal  $p\text{CH}_4$  could be misestimated by up to 64.5%. Shallower systems displayed the most temporal variability in  $p\text{CH}_4$  and waterbodies with more vegetation cover had lower temporal

\*Correspondence: [ner35@cornell.edu](mailto:ner35@cornell.edu)

Additional Supporting Information may be found in the online version of this article.

**Author Contribution Statement:** M.A.H. and D.C.R. conceived the study. M.A.H., M.R.A., J.B., L.E.B., M.F., I.K., A.L., C.M., J.P.M., M.P., D.C.R., J.A., S.B., K.C., M.K., A.R.S., and F.S. took part in sample collection and analysis. N.E.R. and M.A.H. analyzed the data and wrote the first draft of the manuscript. All authors edited and provided feedback on the draft and approve of the final submitted manuscript.

variability. Inland waters remain one of the most uncertain components of the global carbon budget; understanding spatial and temporal variability will ultimately help us to constrain our estimates and inform research priorities.

Lentic waterbodies play a major role in global carbon dioxide (CO<sub>2</sub>) and methane (CH<sub>4</sub>) cycling (Tranvik et al. 2009; Raymond et al. 2013; Rosentreter et al. 2021a). The smallest of these systems (i.e., ponds) have a particularly outsized influence on global and regional CO<sub>2</sub> and CH<sub>4</sub> budgets relative to larger waterbodies due both to high emissions rates and their ubiquity (Holgerson and Raymond 2016; Ollivier et al. 2019). Despite consensus regarding their importance, global estimates of CO<sub>2</sub> and CH<sub>4</sub> emissions from small aquatic systems are among the most uncertain in global budgets (Canadell et al. 2021) and remain highly variable for several reasons (Raymond et al. 2013; Holgerson and Raymond 2016; Rosentreter et al. 2021a). First, the exact number of ponds and shallow lakes remains unclear due to limitations in mapping ability (Messager et al. 2016), but there are likely billions of these systems globally (Downing 2010). Second, each system differs in physical, chemical, and biological properties that affect rates of CO<sub>2</sub> and CH<sub>4</sub> exchange with the atmosphere (Laurion et al. 2010; Holgerson and Raymond 2016; Grinham et al. 2018). Third, there is unknown—and often unaccounted for—spatial and temporal variability in dissolved CO<sub>2</sub> and CH<sub>4</sub> concentrations in the surface waters of ponds and shallow lakes.

Considerable progress has been made in understanding the importance of, and controls on, lentic CO<sub>2</sub> and CH<sub>4</sub> cycling and exchange with the atmosphere across space and time (Schilder et al. 2013; Vachon and Prairie 2013; Rudberg et al. 2021). However, the importance of spatial and temporal variability in the smallest of these systems are not as well constrained, and it is even less clear what physical, biological, and chemical properties might be useful for predicting the most variable systems. One of the primary reasons for this lack of understanding is inconsistent sampling protocols, specifically regarding the intensity of spatial and temporal replication. Testing if variables that can predict dissolved CO<sub>2</sub> and CH<sub>4</sub> concentrations can also predict whether a waterbody will have high or low spatial and temporal variability of CO<sub>2</sub> and CH<sub>4</sub> concentrations is an important step in improving our understanding of CO<sub>2</sub> and CH<sub>4</sub> dynamics in small lentic systems and can inform sampling schemes. Determination of the magnitude of error associated with limited sampling will demonstrate whether it is necessary to sample waterbodies across space and time in order to reduce uncertainty in estimating diffusive CO<sub>2</sub> and CH<sub>4</sub> exchange with the atmosphere and inform methods to improve global upscaling efforts (Wik et al. 2016; Natchimuthu et al. 2017; Loken et al. 2019).

Dissolved CO<sub>2</sub> and CH<sub>4</sub> concentrations vary spatially in larger lentic systems (i.e., lakes and reservoirs; Pacheco et al. 2015; Colas et al. 2020; Praetzel et al. 2021). For example, spatial variation in *p*CO<sub>2</sub> was linked with indicators of planktonic primary

production (i.e., dissolved O<sub>2</sub> concentration, pH) while spatial variation in *p*CH<sub>4</sub> was better described by depth and pH in large (> 12 km<sup>2</sup>) constructed Brazilian reservoirs (Paranaíba et al. 2018). Littoral areas of lakes typically have higher CH<sub>4</sub> concentrations than the pelagic zone (Hoffmann et al. 2013; Schmiedeskamp et al. 2021), though CH<sub>4</sub> emissions might be highest in the center of small waterbodies due to ebullition (Matveev et al. 2016; Schmiedeskamp et al. 2021). In larger waterbodies, differences in gas transfer velocity across space might also lead to variability in dissolved CO<sub>2</sub> and CH<sub>4</sub> concentrations (Schilder et al. 2013). In small, shallow waterbodies, there is less space in which physical, chemical, and biotic drivers of CO<sub>2</sub> and CH<sub>4</sub> concentration can vary, and thus spatial variability of CO<sub>2</sub> and CH<sub>4</sub> in ponds and shallow lakes might be relatively less important than in larger, deeper waterbodies. However, if there is substantial spatial variability in CO<sub>2</sub> and CH<sub>4</sub> concentration in ponds and shallow lakes, sampling schemes that only measure from a single location in the waterbody are likely to misestimate concentration or emission.

Temporal variability in dissolved gas concentrations and diffusive fluxes in larger lentic systems exists across diel (Podgrajsek et al. 2014, 2015; Sieczko et al. 2020), weekly (Colas et al. 2020; Waldo et al. 2021), seasonal (Natchimuthu et al. 2017; Wik et al. 2018; Paranaíba et al. 2021), and annual time frames (Finlay et al. 2019; Colas et al. 2020). Small lentic systems have similar temporal variability to larger lentic systems (Torgersen and Branco 2008; Huotari et al. 2009; Rudberg et al. 2021), but less is known about the controls of this variability as research focus has been on quantifying the magnitude, rather than the drivers, of diel and seasonal CO<sub>2</sub> and CH<sub>4</sub> dynamics (Wik et al. 2016; Natchimuthu et al. 2017; Waldo et al. 2021). We anticipate temporal variability in CO<sub>2</sub> and CH<sub>4</sub> concentrations in shallow lentic systems is likely to be higher than in larger and deeper systems due to more frequent and extreme changes in chemical (e.g., nutrient loading events) and physical factors (e.g., mixing events) that might be linked with CO<sub>2</sub> and CH<sub>4</sub> production and consumption.

Although previous efforts have quantified the importance of spatial and temporal variability in dissolved CO<sub>2</sub> or CH<sub>4</sub> concentration in one or just a few waterbodies, a broader analysis considering many waterbodies across a broad geographic range is needed to determine the prevalence of spatial and temporal variability across systems and to identify possible relationships with environmental variables that might be useful for predicting the most variable systems. In this study, we examined dissolved CO<sub>2</sub> and CH<sub>4</sub> concentrations in 30 shallow lentic waterbodies (i.e., ponds and shallow lakes) across temperate regions of Europe and North America. We aimed to:

(1) identify the main predictors of CO<sub>2</sub> and CH<sub>4</sub> concentrations for shallow waterbodies over a wide geographic scale; (2) quantify the spatial and temporal variability of dissolved CO<sub>2</sub> and CH<sub>4</sub> concentrations in these waterbodies, and determine how limited sampling in space and time might lead to misestimation of mean dissolved CO<sub>2</sub> and CH<sub>4</sub> concentrations; (3) identify waterbody characteristics that can be used to predict systems that are likely to have high spatial and temporal variability in CO<sub>2</sub> and CH<sub>4</sub> concentrations. This work is an important step in advancing our understanding of lentic CO<sub>2</sub> and CH<sub>4</sub> emissions, moving from identification of global emission patterns to reducing confidence intervals and uncertainty associated with these patterns (Downing 2009), helping to reduce uncertainty in global CH<sub>4</sub> emissions estimates.

## Methods

### Sampling locations and scheme

We sampled 30 ponds and shallow lakes in temperate areas of Europe and North America in summer 2018 and 2019 (June–September, though four sampling events took place in October; Fig. 1). Although there are various definitions of ponds and shallow lakes (Biggs et al. 2005), here we use the following: ponds have < 5 ha surface area and < 5 m maximum depth, while shallow lakes have > 5 ha surface area and < 5 m maximum depth (Scheffer 2004; Richardson et al. 2022). The waterbodies we sampled all had permanent hydroperiods and sediment bottoms. They were located in urban parks, residential areas, forests, and agricultural areas. Dissolved gas sampling at each site was conducted on three occasions (except Mud Pond, which was only sampled twice), spread across 61.7 d on average ( $\pm 25.6$  SD), ranging from 33 to 128 d between the first and last sampling date.

We measured waterbody surface area, perimeter, fetch, maximum depth, dissolved organic carbon (DOC), total phosphorus (P), dissolved P concentration, chlorophyll *a* (Chl *a*), conductivity, pH, Secchi depth, emergent plant cover, submerged plant cover, floating plant cover, and the presence or absence of fish. In some waterbodies, these environmental variables were measured once, while at other waterbodies we took the mean value from multiple sample dates. Chemical samples (i.e., DOC, total P, dissolved P, Chl *a*) were characterized using a variety of techniques, employing standard methods in the laboratory that collected the samples (Supporting Information Table S1). Not all variables were measured in all waterbodies or on all sampling occasions (Table 1; Supporting Information Table S1). However, for systems where chemical samples were collected on multiple occasions, within site variability was negligible compared to between site variability.

To test relationships among environmental variables, we used Pearson correlations (Supporting Information Table S2). Prior to estimating correlations and regressions, we checked whether the data distribution for each variable best fit a normal

or lognormal distribution using the *fitdistrplus* package (Delignette-Muller et al. 2015), and made necessary transformations (Table 1). All statistical tests were conducted in R Statistical Software (R Core Team 2014) and we considered the results of statistical tests to be nominally significant (i.e., indicative of relationships that might be useful for explaining variation in the data) when  $p \leq 0.05$ .

### Dissolved gas sampling, analysis, and calculation of partial pressures

Gas sampling was conducted in the same way at all waterbodies, with samples collected from three locations in each waterbody on three occasions (in Gibson Pond and Mud Pond, samples were only collected from the waterbody center). On each sampling date, both air and dissolved gas samples were collected. Air samples ( $n = 2$ ) were collected from  $\sim 0.5$  m above the water surface in the center of the waterbody using syringes that were flushed with air three times prior to sample collection. Air samples were injected into pre-evacuated 12-mL glass exetainers (LabCo Limited). Dissolved gas concentrations were determined using a headspace equilibration technique (McAuliffe 1971; Holgerson 2015; Aho and Raymond 2019), and the headspace samples were stored in pre-evacuated glass exetainers. Two samples were collected from the waterbody center, and an additional sample was collected from each of two site margins (i.e., locations on opposite ends of the waterbody). Samples from the waterbody center were considered as technical replicates, and the average CO<sub>2</sub> and CH<sub>4</sub> concentration of these two samples was used in statistical analyses (we tested variability between the technical replicates as described later in the methods). All dissolved gas samples were collected from surface water by filling a syringe at < 15 cm depth. The temperature of both air and water was measured during sample collection. Atmospheric pressure was determined by the elevation of the waterbody above sea level.

Gas samples were analyzed at the Yale Analytical and Stable Isotope Center using a Shimadzu GC 2014 or at the University of Stirling using a Hewlett Packard GC 5890 Series II. Both instruments were equipped with a flame ionization detector for measuring CH<sub>4</sub>. Sample CO<sub>2</sub> and CH<sub>4</sub> concentrations were determined by comparing sample peak area against a standard curve of the peak areas of different concentrations of external standards. Dissolved CO<sub>2</sub> and CH<sub>4</sub> concentrations were then calculated for each sample following Henry's law and the ideal gas law using constants determined by Weiss (1974) and Wiesenburg and Guinasso (1979).

We converted dissolved gas concentrations to partial pressures ( $pX$ ;  $\mu\text{atm}$ ) using the following equation as presented by Aho and Raymond (2019) where  $[X]$  is the dissolved gas concentration ( $\mu\text{mol L}^{-1}$ ) and  $K_{h,x}$  is Henry's law solubility constant ( $\text{mol L}^{-1} \text{atm}^{-1}$ ) for CO<sub>2</sub> (Weiss 1974) or CH<sub>4</sub> (Wiesenburg and Guinasso 1979) given the temperature the water sample was collected:



**Fig. 1.** Locations of the 30 waterbodies sampled in this study (A), with panels showing location of waterbodies in North America (B) and Europe (C).

$$pX = \frac{[X]}{K_{h,x}} \quad (1)$$

We elected to present gas partial pressures to allow for simple prediction of whether a given location in a waterbody on a specific date is likely to be a source ( $pX >$  atmospheric  $[X]$ ), or sink ( $pX <$  atmospheric  $[X]$ ) of  $\text{CO}_2$  or  $\text{CH}_4$ .

#### Environmental variables related to $p\text{CO}_2$ and $p\text{CH}_4$

We used both univariate and multivariate approaches to identify the best predictors and models of  $p\text{CO}_2$  and  $p\text{CH}_4$  as some environmental variables had low sample sizes (Table 1). We used

univariate linear regressions to identify the strength of the relationship between each chemical, physical, and biological variable measured and mean summer (all gas samples per waterbody)  $p\text{CO}_2$  and  $p\text{CH}_4$  for shallow lentic systems across a broad geographic range. Before calculating regressions, we checked distributions of  $p\text{CO}_2$  and  $p\text{CH}_4$ , again using the *fitdistrplus* package; the mean of all  $p\text{CO}_2$  values was normally distributed, while the mean of all  $p\text{CH}_4$  values was log normally distributed. We excluded Secchi depth from our analyses as it was strongly correlated with several other variables (maximum depth, DOC, total P, Chl *a*) and in several instances Secchi depth was unmeasurable as it was greater than waterbody maximum depth.

**Table 1.** Characteristics of 30 ponds and shallow lakes in temperate areas of Europe and North America in the summers of 2018 and 2019 sampled as part of this study. Waterbody-specific values can be accessed in the data file available online.

Characteristic	n	Data distribution	Mean	Median	Range
Latitude ( $^{\circ}$ N)	30	Log-normal	49.95	46.64	41.69–60.02
Surface area ( $m^2$ )	30	Log-normal	305,240	6227	180–8,230,000
Perimeter (m)	30	Log-normal	898	403	58–11,070
Fetch (m)	30	Log-normal	325.4	177.5	20.0–3190.0
Max depth (m)	30	Log-normal	1.6	1.3	0.6–4.8
Dissolved organic carbon ( $mg\ L^{-1}$ )	28	Log-normal	10.8	7.8	4.8–32.5
Total phosphorus ( $\mu g\ L^{-1}$ )	10	Log-normal	100.9	16.4	3.0–294.0
Dissolved phosphorus ( $\mu g\ L^{-1}$ )	11	Log-normal	63.8	22.5	13.7–236.6
Chl <i>a</i> ( $\mu g\ L^{-1}$ )	20	Log-normal	32.7	22.5	7.2–97.0
Conductivity ( $\mu s\ cm^{-1}$ )	29	Log-normal	397.1	270.6	8.0–1722.0
pH	29	Normal	7.7	7.5	4.5–9.3
Secchi depth (m)	16	Normal	0.89	0.81	0.05–1.83
Emergent cover (% area)	24	Normal	12	10	0–40
Submerged cover (% area)	24	Normal	43	50	0–100
Floating cover (% area)	27	Normal	26	10	0–100
Fish (presence/absence)	30		15 present, 15 absent		

Next, we used multiple linear regression models, stepwise modeling, and an information theoretic model selection approach to determine the best-approximating model to describe mean  $pCO_2$  and  $pCH_4$ . The base model included variables measured in  $n \geq 28$  waterbodies. As several variables measured were strongly correlated with each other, we selected the variable with the largest sample size to include in the model, or if sample size was the same, we selected the variable that was significant in univariate regressions. Thus, the base model consisted of the following fixed effects: maximum depth, pH, DOC, fish presence, and one of surface area, perimeter, or fetch. Including DOC in all models slightly reduced our sample size as it was not measured in two waterbodies, but we elected to include it due to past evidence it is linked with aquatic  $CO_2$  and  $CH_4$  cycling (Deemer and Holgerson 2021; Peacock et al. 2021). For  $pCO_2$ , the base model included the following fixed effects: fetch, maximum depth, DOC, pH, and fish presence. We compared all combinations of fixed effects in this model by calculating Akaike information criterion scores corrected for small sample sizes (AICc) via the dredge function in the *MuMin* package (Barton 2020). We considered the best-approximating model to have the lowest AICc value, and considered models within  $2 \Delta AICc$  ( $\Delta AICc$  being the difference between the best-approximating and lower-ranked models) to be well supported (Burnham and Anderson 2002). We report models within  $2 \Delta AICc$  but do not interpret effects from those containing uninformative parameters (Arnold 2010). If the best-approximating model contained imprecisely estimated covariate effects (i.e., the ratio of the estimated effect to standard error was  $< 2$ ), we only interpreted meaningful effects and advanced well estimated effects to subsequent modeling stages. To this model we then iteratively

added Chl *a*, % floating cover, and % emergent cover (at the cost of reduced df) to see if their inclusion would reduce AICc (recalculated for the inclusion of each new variable owing to changing sample sizes). We repeated this same process for  $pCH_4$ , replacing fetch with surface area, as surface area had a higher  $R^2$  than univariate models of perimeter or fetch. For all models, the fixed effects were scaled and fluxes log transformed in order for models to converge. Neither total P nor dissolved P were included in mixed effect model comparison due to their relatively small sample sizes.

#### Spatial variability in $pCO_2$ and $pCH_4$

To determine the importance of spatial variability and sampling location within a waterbody, we considered the degree to which collecting samples from a single location in a waterbody might misestimate waterbody mean  $pCO_2$  or  $pCH_4$  from three sample locations using a bootstrap regression approach. We built the bootstrap model to randomly select a  $pCO_2$  or  $pCH_4$  value from a single sampling location in the waterbody on a given date as the response variable and the waterbody mean  $pCO_2$  and  $pCH_4$  on that date as the independent variable. We ran 1000 iterations of this model. We did not include waterbody as a random effect in our model despite repeated sampling as it prevented various iterations of the model from converging. Although exclusion of this random effect might be problematic when constructing a model with the goal of most accurately quantifying an  $R^2$  and  $p$ -value, our goal here was to quantify  $\beta$ , or the slope of the regression model. This  $\beta$  value is unlikely to be altered in such a magnitude to influence our interpretation of the model results regardless of the inclusion of the random effect.

We calculated a potential misestimate of waterbody  $p\text{CO}_2$  or  $p\text{CH}_4$  using the 95% confidence interval of slopes estimated in the bootstrap regression (Eq. 2).

$$\text{Potential \% Misestimate} = \frac{|2.5\% \text{ Quantile} - 1| + |97.5\% \text{ Quantile} - 1|}{2} \times 100 \quad (2)$$

The calculated potential misestimate indicates by how much the mean  $p\text{CO}_2$  or  $p\text{CH}_4$  of the water body might be misestimated by sampling from a single location in the water body on a given sampling event. It can be interpreted as the 95% likelihood of a single sample location in the waterbody being within  $X\%$  of the mean waterbody  $p\text{CO}_2$  or  $p\text{CH}_4$  on that sampling date.

Before testing for relationships between environmental variables and spatial variability of  $p\text{CO}_2$  or  $p\text{CH}_4$ , we determined whether variability (as standard deviation [SD]) among samples collected over space was greater than variability of the center technical replicates, in effect testing whether any spatial variability we measured was greater than pure error. In over 85% of the samples for both  $p\text{CO}_2$  and  $p\text{CH}_4$ , the variability in center replicates was less than variability across the three sampling locations in the waterbody (71 out of 84 for  $p\text{CO}_2$  and 74 out of 84 for  $p\text{CH}_4$ ; Supporting Information Fig. S2) when samples were collected at multiple locations. When technical variability was higher than variability across sampling locations within a waterbody, it was typically when mean  $p\text{CO}_2$  or  $p\text{CH}_4$  was low (and thus any variability among technical replicates would appear greater) or the spatial variability was low relative to the mean. As such, our sampling approach accurately reflects spatial variability and is not instead driven by pure error.

To estimate the relative spatial variability of  $p\text{CO}_2$  or  $p\text{CH}_4$  in waterbodies, we used residuals of the linear relationship  $\log(\text{SD}_{p\text{CO}_2} \text{ or } p\text{CH}_4) \sim \log(\text{mean}_{p\text{CO}_2} \text{ or } p\text{CH}_4)$  for each waterbody on each sampling day (Supporting Information Fig. S2). We then used univariate linear mixed effects models to test the relationship between each waterbody characteristic and the  $p\text{CO}_2$  or  $p\text{CH}_4$  residual, with waterbody as a random effect. Models were constructed using the *lme4* and *lmerTest* packages (Bates et al. 2015; Kuznetsova et al. 2017). Conditional and marginal  $R^2$  values for each model were calculated using the *sjstats* package (Lüdecke 2021). Two ponds (Gibson Pond and Mud Pond) were excluded from the spatial variability analysis as sampling was only conducted in the waterbody center. We also conducted a multivariate analysis to identify the best combination of variables to use to identify systems that might be more or less variable following the same approach described previously for mean  $p\text{CO}_2$  or  $p\text{CH}_4$ , but instead using linear mixed effects models with the addition of waterbody as a random effect to account for repeated measures.

### Temporal variability in $p\text{CO}_2$ and $p\text{CH}_4$

We used a similar bootstrap approach as described for spatial variability to quantify the uncertainty in mean  $p\text{CO}_2$  and

$p\text{CH}_4$  associated with sampling each waterbody only once. In the bootstrap regression we used the waterbody mean  $p\text{CO}_2$  or  $p\text{CH}_4$  on a randomly selected date as the response variable and mean of all  $p\text{CO}_2$  or  $p\text{CH}_4$  values from three sampling dates in that waterbody as the independent variable. Potential misestimate of  $p\text{CO}_2$  or  $p\text{CH}_4$  is determined using Eq. 2. It can be interpreted as the 95% likelihood of a single  $p\text{CO}_2$  or  $p\text{CH}_4$  sampling event being within  $X\%$  of the mean  $p\text{CO}_2$  or  $p\text{CH}_4$  of three summer sampling events. We repeated the bootstrap approach a third time, using a random, single sample from each waterbody compared against the mean of all samples collected in space and time to calculate the potential misestimate of mean summer  $p\text{CO}_2$  or  $p\text{CH}_4$  from a single grab sample.

We used similar univariate and multivariate approaches to identify predictors of temporal variability as described previously for mean  $p\text{CO}_2$  or  $p\text{CH}_4$  and spatial variability in  $p\text{CO}_2$  or  $p\text{CH}_4$ , but here we calculated residuals for  $p\text{CO}_2$  and  $p\text{CH}_4$  for each waterbody using the mean  $p\text{CO}_2$  and  $p\text{CH}_4$  from each of the samples collected per waterbody on each sampling date (Supporting Information Fig. S3) and again used multiple linear regression. One pond (Mud Pond) was only sampled twice and was therefore excluded from these calculations.

## Results

### Waterbody characteristics

The sampled ponds and shallow lakes had a large range of physical, chemical, and biological characteristics (Table 1). There were several significant correlations between these characteristics (Supporting Information Table S2), including strong positive correlations between perimeter, fetch, and surface area ( $r \geq 0.90$ ,  $p < 0.01$ ). Notably, surface area and maximum depth were not correlated ( $r = -0.07$ ;  $p = 0.71$ ;  $df = 28$ ). The two largest waterbodies (22 Bay and Simpson Bay;  $> 100,000 \text{ m}^2$ ) and three smallest (E4, Fizzy, Karls Pond;  $< 1000 \text{ m}^2$ ) all have a similar maximum depth (0.64–1.25 m). The system with the greatest maximum depth was Lost Pond (4.8 m) which has a surface area ( $6354 \text{ m}^2$ ) similar to the dataset median ( $6227 \text{ m}^2$ ).

### Environmental variables related to $p\text{CO}_2$ and $p\text{CH}_4$

On average, waterbodies had mean  $p\text{CO}_2$  ( $3094 \pm 3576 \mu\text{atm}$ ; mean  $\pm$  SD; Fig. 2a) nearly 7 $\times$  higher than the mean  $p\text{CO}_2$  of air samples ( $446.0 \pm 40.0 \mu\text{atm}$ ) indicative of supersaturation and net release of  $\text{CO}_2$  to the atmosphere. Six waterbodies had mean  $p\text{CO}_2$  below atmospheric concentration on all three sampling events indicating they were net  $\text{CO}_2$  sinks. Eight waterbodies had variable source-sink behavior across sampling dates, and several had variable source-sink behavior at different locations in the system on individual sampling dates.  $p\text{CH}_4$  ranged across several orders of magnitude from a low of  $199.5 \mu\text{atm}$  in Simpson Bay to a

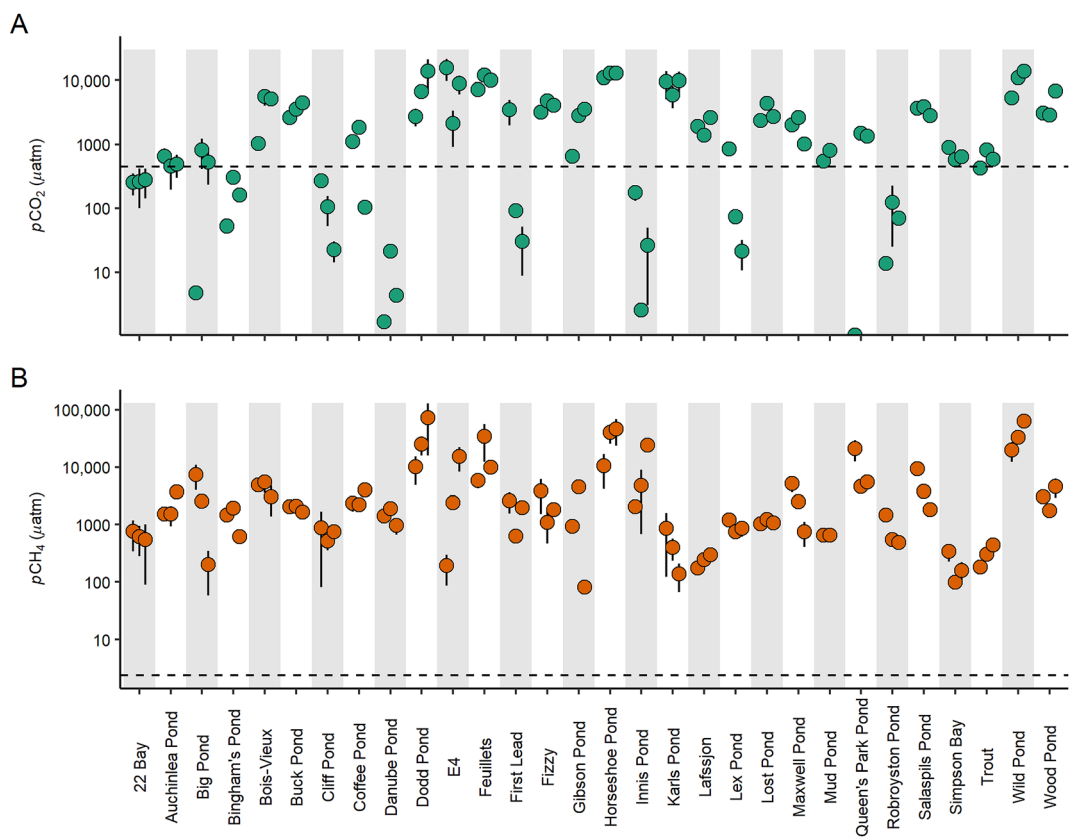


**Fig. 2.** Partial pressures of carbon dioxide (A;  $p\text{CO}_2$ ) and methane (B;  $p\text{CH}_4$ ) in surface water of 30 ponds and shallow lakes in temperate areas of Europe and North America. Measurements were made in the summers of 2018 and 2019. Each point indicates mean gas partial pressure in a single waterbody on a single sampling date. The error bars represent the SD in  $p\text{CO}_2$  or  $p\text{CH}_4$  in space on that sampling date. Dashed lines indicate mean atmospheric gas concentration across all sampling events with points above the line indicative of gas release to the atmosphere and points below indicative of uptake by the waterbody. In cases where error bars are hidden, the SD is very small (there is no SD for Gibson Pond or Mud Pond as samples were collected from a single location in these waterbodies).

high of  $38,803\ \mu\text{atm}$  in Wild Pond, though all systems had partial pressures of  $\text{CH}_4$  (mean  $p\text{CH}_4 = 6350 \pm 10,578\ \mu\text{atm}$ ; Fig. 2B) higher than the atmosphere ( $2.43 \pm 0.66\ \mu\text{atm}$ ) across all sampling dates and sampling locations. Generally, waterbodies with high mean  $p\text{CO}_2$  had high mean  $p\text{CH}_4$  (Supporting Information Fig. S1).

We identified several physical and biological variables that related to  $p\text{CO}_2$  and  $p\text{CH}_4$  (Supporting Information Table S9; Fig. 3). Waterbodies with smaller surface areas had higher  $p\text{CO}_2$  ( $r^2 = 0.25$ ;  $p = 0.01$ ;  $df = 28$ ) and  $p\text{CH}_4$  ( $r^2 = 0.16$ ;  $p = 0.03$ ;  $df = 28$ ) than those with larger surface areas. The percent area of the waterbody covered in floating vegetation positively related to both  $p\text{CO}_2$  ( $r^2 = 0.32$ ;  $p < 0.01$ ;  $df = 25$ ) and  $p\text{CH}_4$  ( $r^2 = 0.22$ ;  $p = 0.01$ ;  $df = 25$ ). Emergent vegetation cover was positively related to  $p\text{CO}_2$  ( $r^2 = 0.27$ ;  $p = 0.01$ ;  $df = 22$ ) but not  $p\text{CH}_4$ . The variable that mostly strongly predicted  $p\text{CO}_2$  was dissolved P concentration ( $r^2 = 0.55$ ;  $p = 0.01$ ;  $df = 9$ ), which had a positive relationship, though the sample size was relatively low ( $n = 11$ ) compared to most other measures. Fish presence related to both  $\text{CO}_2$  and  $\text{CH}_4$  concentrations:  $p\text{CO}_2$  was

almost four times higher in fishless systems ( $4765 \pm 4272\ \mu\text{atm}$   $\text{CO}_2$ ) than in those with fish ( $1423 \pm 1502\ \mu\text{atm}$   $\text{CO}_2$ ;  $p < 0.01$ ;  $df = 28$ ) and  $p\text{CH}_4$  was nearly five times greater in fishless systems ( $10,545 \pm 13,688\ \mu\text{atm}$   $\text{CH}_4$ ) relative to those with fish ( $2156 \pm 2597\ \mu\text{atm}$   $\text{CH}_4$ ;  $p = 0.03$ ;  $df = 28$ ).

The best-approximating multivariate model to describe waterbody mean  $p\text{CO}_2$  included DOC ( $\beta = 0.28$ ;  $SE = 0.02$ ), fish presence ( $\beta = -0.72$ ;  $SE = 0.29$ ), and pH, but the pH effect was not well estimated ( $\beta = -0.27$ ;  $SE = 0.14$ ;  $R^2 = 0.30$ ;  $p < 0.01$ ;  $df = 25$ ; Supporting Information Table S3). The addition of various primary producers did not improve the model's ability to predict mean  $p\text{CO}_2$  (Supporting Information Table S3). The best-approximating multivariate model to describe waterbody mean  $p\text{CH}_4$  was fish presence alone ( $\beta = -0.57$ ;  $SE = 0.22$ ; Supporting Information Table S4). The addition of Chl  $a$  did not improve the model, but the addition of floating and submerged plant cover did (Supporting Information Table S4). Floating plant cover was positively associated with  $p\text{CH}_4$  ( $\beta = 0.25$ ;  $SE = 0.11$ ) as was submerged plant cover ( $\beta = 0.27$ ;  $SE = 0.12$ ).

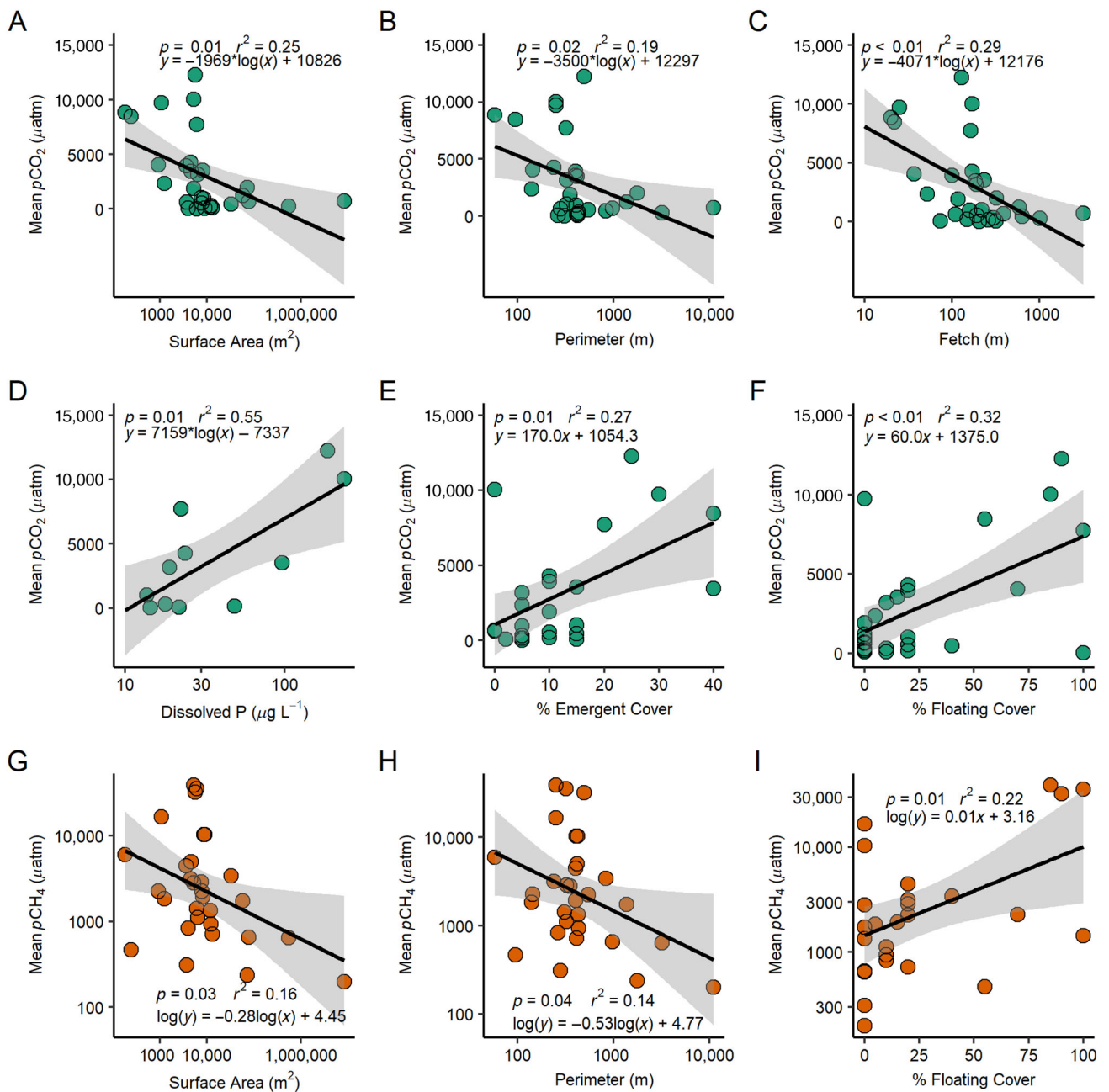


**Fig. 3.** Relationships between mean partial pressures of carbon dioxide ( $p\text{CO}_2$ ) and waterbody (A) surface area, (B) perimeter, (C) fetch, (D) dissolved phosphorus concentration, (E) emergent cover, and (F) floating cover, and between partial pressures of methane ( $p\text{CH}_4$ ) and waterbody (G) surface area, (H) perimeter, and (I) floating cover. Only relationships with  $p \leq 0.05$  shown, other relationships with  $p > 0.05$  in Supporting Information Table S9. Measurements were made in 30 ponds and shallow lakes in temperate areas of Europe and North America in the summers of 2018 and 2019.

### Spatial variability in $p\text{CO}_2$ and $p\text{CH}_4$

Bootstrap regressions indicated that randomly sampling from a single location in small waterbodies results in low (13%) misestimates in  $p\text{CO}_2$  (Table 2). This relatively low spatial variability in  $p\text{CO}_2$  was further evidenced by the lack of any environmental variables that were significantly correlated with  $p\text{CO}_2$  residuals (Supporting Information Table S10). There was slightly more spatial variability in  $p\text{CH}_4$  (35%

potential misestimate in space; Table 2), and we found that spatial variability was negatively correlated with water depth ( $R^2 = 0.13, p < 0.01, n = 84$ ; Fig. 4A), and positively correlated with Chl *a* concentration ( $R^2 = 0.08, p = 0.05, n = 57$ ; Fig. 4B) and conductivity ( $R^2 = 0.08, p = 0.02, n = 81$ ; Fig. 4C). Using a multivariate approach, the best model to approximate  $p\text{CO}_2$  variability in space was the null model ( $R^2 = 0.00, p = 0.17, n = 81$ ; Supporting Information Table S5), while the best

**Table 2.** Results of bootstrap regressions ( $n = 1000$  iterations) of randomly sampled partial pressures of carbon dioxide ( $p\text{CO}_2$ ) or methane ( $p\text{CH}_4$ ) in space and time relative to mean  $p\text{CO}_2$  or  $p\text{CH}_4$ . “Space” refers to selecting a  $p\text{CO}_2$  or  $p\text{CH}_4$  value from a single location in the waterbody relative to the waterbody mean  $p\text{CO}_2$  or  $p\text{CH}_4$  on a given date, “Time” refers to randomly selecting waterbody mean  $p\text{CO}_2$  or  $p\text{CH}_4$  on a single date relative to the seasonal mean  $p\text{CO}_2$  or  $p\text{CH}_4$ , and “Time and Space” refers to selecting a single  $p\text{CO}_2$  or  $p\text{CH}_4$  sample as representative of the seasonal mean. Potential misestimate is calculated as described in Eq. 3. Measurements were made in 30 ponds and shallow lakes in temperate areas of Europe and North America in the summers of 2018 and 2019.

	$R^2$	$p$ -value	Mean intercept	Intercept 95% CI	Mean slope	Slope 95% CI	Min. slope	Max. slope	Potential % misestimate
Space $p\text{CO}_2$	0.92	< 0.01	-2.17	-217.2 to 245.8	1.00	0.87–1.13	0.83	1.16	13
Space $p\text{CH}_4$	0.90	< 0.01	-37.37	-1302 to 1370	1.00	0.63–1.33	0.56	1.44	35
Time $p\text{CO}_2$	0.90	< 0.01	7.75	-396.2 to 410.3	0.99	0.73–1.25	0.61	1.33	26
Time $p\text{CH}_4$	0.93	< 0.01	3.91	-2123 to 1829	0.99	0.39–1.68	0.35	1.76	64.5
Time and Space $p\text{CO}_2$	0.92	< 0.01	-0.19	-403.0 to 423.3	1.00	0.72–1.31	0.62	1.50	44
Time and Space $p\text{CH}_4$	0.87	< 0.01	-17.96	-3015 to 2236	0.99	0.36–2.03	0.21	2.42	83.5

model to describe variability of  $p\text{CH}_4$  in space was maximum depth alone ( $\beta = -0.13$ ;  $\text{SE} = 0.05$ ; Supporting Information Table S6). Primary producers did not improve either model (Supporting Information Tables S5, S6).

#### Temporal variability in $p\text{CO}_2$ and $p\text{CH}_4$

The variability of dissolved gas concentrations was greater in time than space. Bootstrap regressions reveal potential misestimation of summer mean  $p\text{CO}_2$  by up to 26% and  $p\text{CH}_4$  by up to 64.5% if sampling is only conducted on a single date (Table 2). Taken a step further, the potential misestimate increases to 44% for  $p\text{CO}_2$  and 83.5% for  $p\text{CH}_4$  (Table 2) if only a single sample from a random location in the waterbody on a single sampling event (the combined effects of spatial and temporal variability) is used to estimate mean summer  $p\text{CO}_2$  or  $p\text{CH}_4$ .

Temporal variability in  $p\text{CO}_2$  was negatively correlated with waterbody perimeter ( $r^2 = 0.11$ ,  $p = 0.05$ ;  $\text{df} = 27$ ; Fig. 5A),

Chl *a* concentration ( $r^2 = 0.21$ ,  $p = 0.03$ ;  $\text{df} = 17$ ; Fig. 5B), and percent emergent cover ( $r^2 = 0.15$ ,  $p = 0.04$ ;  $\text{df} = 21$ ; Fig. 5C). There was no relationship between temporal variability in  $p\text{CO}_2$  and the length of time between the first and last sampling event. Temporal variability of  $p\text{CH}_4$  decreased as the waterbody maximum depth ( $r^2 = 0.18$ ,  $p = 0.01$ ;  $\text{df} = 27$ ; Fig. 5D) and percent submerged cover increased ( $r^2 = 0.20$ ,  $p = 0.02$ ;  $\text{df} = 21$ ; Fig. 5E), and was positively correlated with sampling time frame ( $r^2 = 0.24$ ,  $p < 0.01$ ;  $\text{df} = 27$ ; Fig. 5F).

The multivariate model with the lowest AICc score for describing variability of  $p\text{CO}_2$  over time was perimeter alone, but the effect of perimeter was not well estimated ( $\beta = -0.11$ ;  $\text{SE} = 0.07$ ; Table S7). The addition of Chl *a* improved the null model, and Chl *a* was negatively correlated with variability of  $p\text{CO}_2$  over time ( $\beta = -0.21$ ;  $\text{SE} = 0.07$ ). Similarly, the addition of emergent cover improved the model and emergent cover was negatively associated with variability of  $p\text{CO}_2$  over time ( $\beta = -0.11$ ;  $\text{SE} = 0.05$ ). Inclusion of floating and submerged

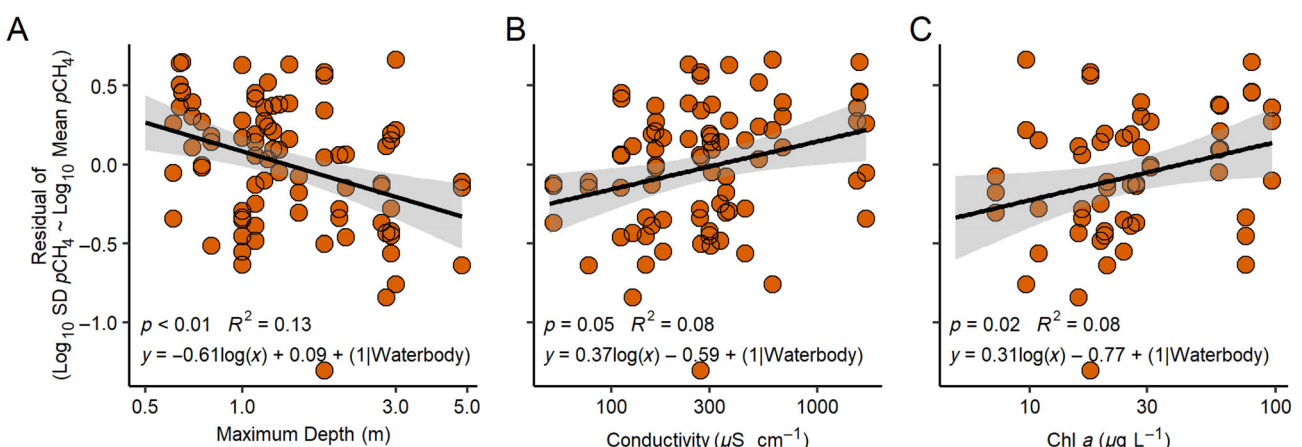


**Fig. 4.** Relationships between spatial variability of the partial pressure of methane ( $p\text{CH}_4$ ) and maximum depth (A), conductivity (B), and Chl *a* (C). Only relationships with  $p \leq 0.05$  shown, other relationships with  $p > 0.05$  in Supporting Information Table S10. The  $(1|\text{Waterbody})$  indicates inclusion of waterbody as a random effect in the model.  $R^2$  values shown are the marginal  $R^2$  of the model. Measurements were made in 30 ponds and shallow lakes in temperate areas of Europe and North America in the summers of 2018 and 2019.

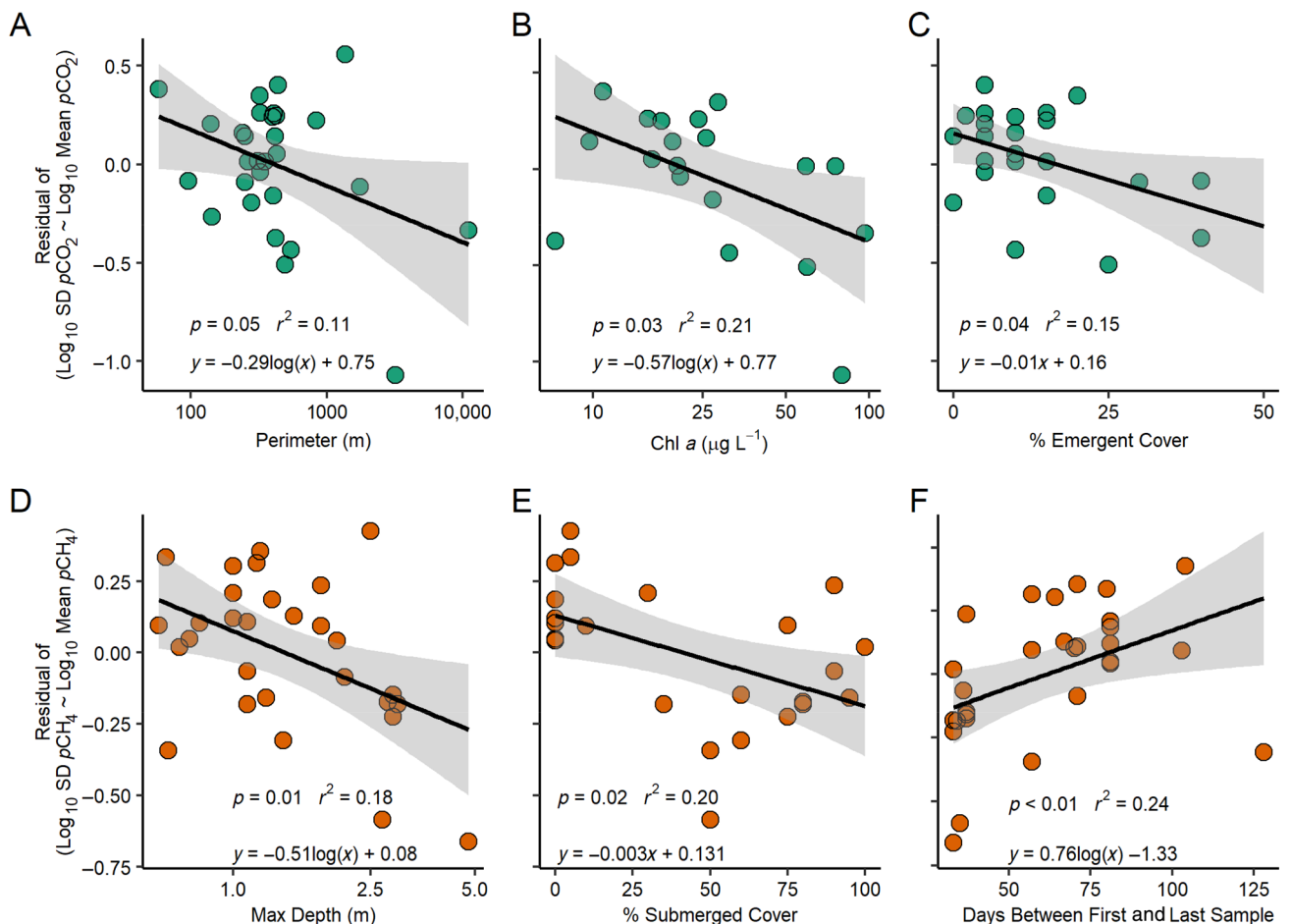


**Fig. 5.** Relationships between temporal variability of the partial pressure of carbon dioxide ( $p\text{CO}_2$ ) and waterbody perimeter (A), Chl  $a$  (B), and % emergent cover (C) and between temporal variability of the partial pressure of methane ( $p\text{CH}_4$ ) and maximum waterbody depth (D), percent submerged cover (E), and the number of days between the first and last sample collected (F). Only relationships with  $p \leq 0.05$  shown, other relationships with  $p > 0.05$  in Supporting Information Table S11. Measurements were made in 30 ponds and shallow lakes in temperate areas of Europe and North America in the summers of 2018 and 2019.

plant cover did not improve the model (Supporting Information Table S7). For temporal variability of  $p\text{CH}_4$  the best-approximating model was maximum depth alone ( $\beta = -0.16$ ;  $\text{SE} = 0.04$ ) and primary producers did not improve the model (Supporting Information Table S8).

## Discussion

Identifying drivers of  $\text{CO}_2$  and  $\text{CH}_4$  concentrations in small and shallow waterbodies is critical for accurate inclusion of these systems in global  $\text{CO}_2$  and  $\text{CH}_4$  budgets. Determining how these systems vary in space and time will guide targeted sampling and further reduce error in our global estimates, and thus improve accuracy in scaling. Here, we found a mix of source/sink behavior for  $p\text{CO}_2$  across waterbodies, sampling dates, and locations within the waterbody, whereas all waterbodies were supersaturated in  $\text{CH}_4$ . Both  $p\text{CO}_2$  and  $p\text{CH}_4$  spanned 4 orders of magnitude across the 30 waterbodies

representing a broad geographic range. We took advantage of this variability to identify relationships between physical, chemical, and biological parameters and  $\text{CO}_2$  and  $\text{CH}_4$  concentration and variability, providing important insight into which systems may be the most variable.

### Environmental variables related to $p\text{CO}_2$ and $p\text{CH}_4$

Despite our focus on shallow and relatively small systems, we still observed inverse relationships between waterbody size (i.e., surface area, fetch, perimeter) and  $p\text{CO}_2$  and  $p\text{CH}_4$  similar to relationships observed across a wider range of waterbody sizes (Holgerson and Raymond 2016; Deemer and Holgerson 2021). In smaller lentic systems it can be unclear whether the negative relationships between size and  $\text{CO}_2$  or  $\text{CH}_4$  concentrations are driven by physical processes or by chemical/biological drivers of  $\text{CO}_2$  or  $\text{CH}_4$  concentration that can co-vary with size. In our dataset there were correlations between waterbody size (i.e., surface area, perimeter, fetch)

and proxies of nutrient and organic matter loading (i.e., DOC, total P, dissolved P concentration), but only dissolved P predicted  $p\text{CO}_2$  and none of the chemical variables measured in this study predicted  $p\text{CH}_4$ . Together, this indicates that physical and biological factors may have a greater effect than chemical factors (or bulk chemical pools) on  $\text{CH}_4$  concentrations in small freshwater systems. This conclusion is supported by evidence from boreal lakes  $< 0.07 \text{ km}^2$  in Finland, where water column stability and turbulent mixing in smaller systems were more important than total organic carbon (TOC) loading from the surrounding landscape in predicting  $\text{CH}_4$  (Kankaala et al. 2013), despite co-variance between lake size and TOC.

Dissolved P concentration had the strongest relationship with  $p\text{CO}_2$ , with highest  $p\text{CO}_2$  when dissolved P concentration was highest (although dissolved P concentration was only measured in 11 waterbodies). Multivariate analysis included DOC and fish presence in the best-approximating model (dissolved P was not included in multivariate analysis due to small sample size). We are unable to determine the underlying mechanisms behind these relationships but can suggest two non-mutually exclusive hypotheses. First, systems with high organic matter loading (whether from internal or external sources) are likely to have high rates of sediment respiration and release of  $\text{CO}_2$ , DOC, and dissolved P to the water column. Second, groundwater and runoff derived dissolved P, DOC, and  $\text{CO}_2$  loaded to small lentic systems could be concurrent (Marcé et al. 2015; Peacock et al. 2019). Jensen et al. (2022) report a positive relationship between DOC and dissolved  $\text{CO}_2$  concentration and a negative relationship between  $\delta^{18}\text{O}$  (indicative of groundwater influence) and dissolved  $\text{CO}_2$  concentration in small agricultural reservoirs, indicating the importance of runoff and groundwater in DOC loading and  $\text{CO}_2$  production.

Vegetation can also regulate  $\text{CO}_2$  and  $\text{CH}_4$  in aquatic systems (Bodmer et al. 2021; Bastviken et al. 2023). We found that the percent of the waterbody covered with floating vegetation related positively to both  $p\text{CO}_2$  and  $p\text{CH}_4$  and the percent of the waterbody area covered with emergent vegetation was positively related to  $p\text{CO}_2$ . Emergent cover had a strong negative correlation with surface area, but the addition of emergent cover to the best-approximating model—which did not include waterbody area—improved the model, hinting that vegetation may be more important than surface area in regulating  $p\text{CO}_2$  in small waterbodies. On the other hand, the areal coverage of floating vegetation was not correlated with any other environmental variables measured (Supporting Information Table S2), indicating a clear effect where floating vegetation increased both  $p\text{CO}_2$  and  $p\text{CH}_4$ . Floating plants can reduce gas exchange between the water column and the atmosphere, preventing diffusion of  $\text{O}_2$  into the water column and allowing for a buildup of  $\text{CO}_2$  and  $\text{CH}_4$  (Goodwin et al. 2008; Kosten et al. 2016; Rabaey and Cotner 2022). Alternatively, floating plants can reduce  $\text{CH}_4$  concentrations in surface water via oxygen loss through their roots and by providing surface

area for methanotrophic bacteria. The balance of reduced diffusion due to physical obstruction with enhanced oxidation via root transfer ultimately dictates how floating vegetation will alter surface water  $\text{CH}_4$  concentrations. In this study, both  $p\text{CO}_2$  and  $p\text{CH}_4$  increased as floating plant cover increased suggesting reduced gas transfer drove this pattern.

Fish presence was an important indicator of average waterbody  $p\text{CO}_2$  and  $p\text{CH}_4$ , which approximately four and five times higher, respectively, in fishless waterbodies compared to those with fish. Although there is evidence that fish can alter aquatic  $\text{CO}_2$  and  $\text{CH}_4$  cycling (Schindler et al. 1997; Atwood et al. 2013; Devlin et al. 2015) it is also possible that fish presence may simply correlate with other factors that regulate  $p\text{CO}_2$  and  $p\text{CH}_4$  (e.g., anoxia-driven winter fish kills). We can conclude that fish presence is a useful variable to measure for predicting  $p\text{CO}_2$  and  $p\text{CH}_4$  in ponds and shallow lakes and more work to quantify how fish alter  $p\text{CO}_2$  and  $p\text{CH}_4$  is needed.

### Spatial variability in $p\text{CO}_2$ and $p\text{CH}_4$

Results of this study support past evidence that spatial variability in lentic systems  $< 10 \text{ km}^2$  may be important for accurate quantification of  $p\text{CH}_4$  (Wik et al. 2016; Natchimuthu et al. 2017), with the possibility of misestimating waterbody mean  $p\text{CH}_4$  by up to 35% if only one location in the waterbody is sampled. Spatial variability in  $p\text{CO}_2$  appears less important in these small waterbodies and accurate estimates of waterbody  $p\text{CO}_2$  can likely be made from a single location.

Only three variables related to the spatial variability of  $p\text{CH}_4$ , and model selection indicates spatial variability of  $p\text{CH}_4$  is best described by the maximum depth of the system, with less variability in deeper waterbodies. We expected the opposite: that deeper systems would be more spatially variable as littoral zones may have greater  $\text{CH}_4$  concentrations than deeper waters (Hofmann 2013; Schmiedeskamp et al. 2021). We can test whether basin shape is related to spatial variability in  $p\text{CH}_4$  using the ratio of surface area to maximum depth. Doing so, we found no relationship between  $p\text{CH}_4$  variability and this ratio (marginal  $R^2 < 0.01$ ). An alternative explanation for the observed negative relationship between depth and spatial variability considers stratification dynamics, which can be associated with maximum depth (Holgerson et al. 2022). Deeper systems with stronger stratification may become anoxic in bottom waters, favoring  $\text{CH}_4$  production, but potentially trapping this  $\text{CH}_4$  beneath the thermocline, with little exchange of  $\text{CH}_4$  with surface waters; in contrast, shallow waters may have both more horizontal and vertical mixing that could create more spatial heterogeneity in  $\text{CH}_4$  concentration. Disruption of stratification is an important driver of spatial variability in  $\text{CH}_4$  concentrations in larger systems (Paranaíba et al. 2018, 2021), and may be similarly important in small lentic systems.

Spatial variability in  $p\text{CH}_4$  increased with Chl  $a$  concentration and conductivity in univariate regressions, but in multivariate analysis, neither was included in the best model. Chl  $a$  may

indicate increased organic matter loading in some areas (with subsequent spatial variability in CH<sub>4</sub> production) or if production is synchronous throughout the waterbody, areas with anoxic conditions may favor slightly higher CH<sub>4</sub> production, again leading to relatively higher spatial variability than systems with lower planktonic primary production.

### Temporal variability in pCO<sub>2</sub> and pCH<sub>4</sub>

The potential for misestimating *p*CO<sub>2</sub> or *p*CH<sub>4</sub> over time was nearly twice the potential of misestimating *p*CO<sub>2</sub> or *p*CH<sub>4</sub> in space and was more important for *p*CH<sub>4</sub> (64.5% potential misestimate) than for *p*CO<sub>2</sub> (26% potential misestimate). Considering only univariate regressions, both *p*CO<sub>2</sub> and *p*CH<sub>4</sub> were associated with waterbody physical and biological characteristics, with greater variability in relatively smaller systems with less primary producer biomass. Temporal variability of *p*CO<sub>2</sub> was associated with perimeter, Chl *a*, and emergent cover, but perimeter was not important when using a multivariate statistical approach. Temporal variability in *p*CH<sub>4</sub> was linked with maximum depth and submerged plant cover, but maximum depth alone was the best-approximating model following multivariate model selection.

Shallower systems had greater temporal variability in *p*CH<sub>4</sub> ( $R^2 = 0.18$ ,  $p = 0.01$ ,  $df = 27$ , Fig. 5D), again hinting at the role of mixing in driving variability. If a waterbody remains stratified or mixes daily throughout the summer, it is likely to display relatively low variability in surface water dissolved CH<sub>4</sub> concentration. Those that mix intermittently (e.g., once a week or once per month) have longer time periods in which dissolved oxygen can be depleted and CH<sub>4</sub> can build, and once mixing occurs, dissipation of this CH<sub>4</sub> will likely take several days, leading to fluctuating periods of high and low surface *p*CH<sub>4</sub>. Maximum depth plays an important role in regulating mixing as deeper waters mix less frequently (Holgerson et al. 2022). Vegetation may also contribute to greater stratification either by blocking wind (emergent vegetation) or through shading and dissipating kinetic wind energy (submerged vegetation; Herb and Stefan 2004; Chimney et al. 2006; Andersen et al. 2017). In our mixed effects models, temporal variability in *p*CH<sub>4</sub> was negatively associated with greater submerged cover (though it did not meet criteria to be considered as an informative parameter). However, this negative relationship hints at vegetation's role in reducing mixing.

We only measured dissolved CH<sub>4</sub> in this study, which contributes to diffusive CH<sub>4</sub> emissions, and it is important to note that there may be similarly high temporal variability in ebullitive CH<sub>4</sub> emissions, which can contribute between 3% and 100% of the total CH<sub>4</sub> flux in waterbodies  $< 0.05 \text{ km}^2$  (estimated using data from Rosentreter et al. 2021b). The same factors that predict temporal variability of dissolved CH<sub>4</sub> are also likely to be important for diffusive CH<sub>4</sub>, with stratification and mixing controlling rates of production of CH<sub>4</sub> that can be released via ebullition, and plants possibly providing a physical block between ebullition and the atmosphere. The

methods we present here may be useful for identifying drivers of spatial and temporal variability in ebullitive CH<sub>4</sub> flux from small waterbodies.

### Implications for future upscaling of small waterbody CO<sub>2</sub> and CH<sub>4</sub> emissions

Understanding drivers of spatial and temporal variability of *p*CO<sub>2</sub> and *p*CH<sub>4</sub> will inform better sampling strategies and help improve models that upscale greenhouse gas emissions from inland waterbodies. Here, we show that *p*CO<sub>2</sub> and *p*CH<sub>4</sub> within small waterbodies vary almost twice as much in time as in space. Furthermore, a single sample from a single location can misestimate mean seasonal *p*CO<sub>2</sub> and *p*CH<sub>4</sub> by up to 44% for *p*CO<sub>2</sub> and up to 83.5% for *p*CH<sub>4</sub>. These misestimates demonstrate the importance of repeated sampling over time, followed by greater spatial coverage in small waterbodies.

There is still debate over the most appropriate sampling resolution in space for accurate estimation of dissolved CO<sub>2</sub> and CH<sub>4</sub> concentrations and diffusive flux with the atmosphere. For example, recent work in tropical reservoirs in Brazil (Paranaiba et al. 2018), a hemiboreal lake in southern Sweden (Natchimuthu et al. 2017), and subarctic lakes in northern Sweden (Wik et al. 2016) recommend between 6 and 300 sampling locations per km<sup>2</sup>. Balancing a reasonable number of samples with accurately incorporating spatial variability is challenging. The low spatial variability of *p*CO<sub>2</sub> in ponds and shallow lakes recorded suggests a single sample can represent the entire waterbody on a given date. As *p*CH<sub>4</sub> was slightly more variable in space, more than one location in the waterbody should be sampled. While improving spatial resolution of CO<sub>2</sub> and CH<sub>4</sub> dynamics in small waterbodies will improve upscaling estimates, this is of secondary importance to improved temporal resolution to improve *p*CO<sub>2</sub> and *p*CH<sub>4</sub> estimates from small lentic systems.

Sampling a waterbody repeatedly over time is necessary to accurately quantify seasonal patterns of dissolved CH<sub>4</sub> and CO<sub>2</sub> concentrations, though this is more important for CH<sub>4</sub> than CO<sub>2</sub>. Most measurements of dissolved gas concentrations and fluxes in temperate systems are made in the summer, and seasonal studies are often limited to a round of sampling in the spring, summer, and fall. This approach misses intra-seasonal variability, in addition to missing the transition period between seasons (i.e., the "shoulder seasons") when important processes such as macrophyte die-off or spring thaw occur. For example, CH<sub>4</sub> emissions over a 2-week period in the late spring accounted for nearly 20% of annual CH<sub>4</sub> emissions from a 2.4 km<sup>2</sup> waterbody (Waldo et al. 2021), and CO<sub>2</sub> and CH<sub>4</sub> emissions during the ice-melt period represent 17% and 27% of annual emissions from northern lakes (Denfeld et al. 2018), highlighting the importance of short time periods between sampling events. Natchimuthu et al. (2017) suggest at least 8 sampling days during the ice-free season are needed to be within 20% of the true measure and Wik et al. (2016) suggest 11 sampling days. We recommend frequent sampling

particularly in smaller systems due to the relationship of increasing temporal variability of  $p\text{CH}_4$  and mean  $p\text{CH}_4$  as system size decreases.

Small and shallow waterbodies are known to release significant quantities of  $\text{CO}_2$  and  $\text{CH}_4$  to the atmosphere (Holgerson and Raymond 2016; Rosentreter et al. 2021a). Here, we have shown that the smallest of these systems also have the highest variability in  $p\text{CO}_2$  and  $p\text{CH}_4$  across space and time. Physical characteristics and dissolved nutrients appear to be the most important variables for understanding both mean  $p\text{CO}_2$  and  $p\text{CH}_4$  and variability of  $p\text{CO}_2$  and  $p\text{CH}_4$  in space and time. Dissolved P concentration is particularly useful for understanding  $\text{CO}_2$  dynamics—we found relationships between dissolved P concentration and mean  $p\text{CO}_2$ , spatial variability in  $p\text{CO}_2$ , and temporal variability in  $p\text{CO}_2$ . Physical features associated with regulation of mixing patterns, such as maximum depth, are important for predicting  $p\text{CH}_4$  and variability in  $p\text{CH}_4$  and merit further investigation. Identifying variables to predict mean  $p\text{CH}_4$  and  $p\text{CO}_2$  and variability of  $p\text{CH}_4$  and  $p\text{CO}_2$  over space and time in small waterbodies will inform future study designs and targeted sampling of variable systems, and also reduce uncertainty in upscaling global greenhouse gas emissions.

### Data Availability Statement

The dataset used in this study can be accessed via the Figshare Repository ([https://figshare.com/articles/dataset/Dataset\\_for\\_Spatial\\_and\\_temporal\\_variability\\_in\\_greenhouse\\_gas\\_partial\\_pressures\\_in\\_shallow\\_lakes\\_and\\_ponds/19495121](https://figshare.com/articles/dataset/Dataset_for_Spatial_and_temporal_variability_in_greenhouse_gas_partial_pressures_in_shallow_lakes_and_ponds/19495121)) and the code used for statistical analysis is available on Github (<https://github.com/nray17/PONDING-GHG-R-Code>).

### References

Aho, K. S., and P. A. Raymond. 2019. Differential response of greenhouse gas evasion to storms in forested and wetland streams. *J. Geophys. Res. Biogeosci.* **124**: 649–662. doi:[10.1029/2018JG004750](https://doi.org/10.1029/2018JG004750)

Andersen, M. R., K. Sand-Jensen, R. Iestyn Woolway, and I. D. Jones. 2017. Profound daily vertical stratification and mixing in a small, shallow, wind-exposed lake with submerged macrophytes. *Aquat. Sci.* **79**: 395–406. doi:[10.1007/s00027-016-0505-0](https://doi.org/10.1007/s00027-016-0505-0)

Arnold, T. W. 2010. Uninformative parameters and model selection using Akaike's information criterion. *J. Wildl. Manage.* **74**: 1175–1178. doi:[10.2193/2009-367](https://doi.org/10.2193/2009-367)

Atwood, T. B., E. Hammill, H. S. Greig, P. Kratina, J. B. Shurin, D. S. Srivastava, and J. S. Richardson. 2013. Predator-induced reduction of freshwater carbon dioxide emissions. *Nat. Geosci.* **6**: 191–194. doi:[10.1038/ngeo1734](https://doi.org/10.1038/ngeo1734)

Barton, K. 2020. MuMin: Multi-model inference. R package version 1.43.17.

Bastviken, D., C. C. Treat, S. Rao, V. Gauci, A. Enrich, M. Karlson, M. Gålfalk, and M. Brandini. 2023. The importance of plants for methane emission at the ecosystem scale. *Aquat. Bot.* **184**: 103596. doi:[10.1016/j.aquabot.2022.103596](https://doi.org/10.1016/j.aquabot.2022.103596)

Bates, D., M. Maechler, B. Bolker, and S. Walker. 2015. Fitting linear mixed-effects models using *lme4*. *J. Stat. Softw.* **67**: 1–48. doi:[10.1126/science.1176170](https://doi.org/10.1126/science.1176170)

Biggs, J., P. Williams, M. Whitfield, P. Nicolet, and A. Weatherby. 2005. 15 years of pond assessment in Britain: Results and lessons learned from the work of Pond Conservation. *Aquat. Conserv. Mar. Freshw. Ecosyst.* **15**: 693–714. doi:[10.1002/aqc.745](https://doi.org/10.1002/aqc.745)

Bodmer, P., R. Vroom, T. Stepina, P. Giorgio, and S. Kosten. 2021. Methane fluxes of vegetated areas in natural freshwater ecosystems: Assessments and global significance. *EarthArXiv*.

Burnham, K., and D. Anderson. 2002. Model selection and multimodel inference: A practical information-theoretic approach. Springer.

Canadell, J. G., and others. 2021. Global carbon and other biogeochemical cycles and feedbacks, p. 673–816. In V. Masson-Delmotte, P. Zhai, A. Pirani, and others [eds.], *Climate change 2021: The physical science basis. Contribution of Working Group I to the Sixth Assessment Report of the Intergovernmental Panel on Climate Change*. Cambridge Univ. Press.

Chimney, M. J., L. Wenkert, and K. C. Pietro. 2006. Patterns of vertical stratification in a subtropical constructed wetland in south Florida (USA). *Ecol. Eng.* **27**: 322–330. doi:[10.1016/j.ecoleng.2006.05.017](https://doi.org/10.1016/j.ecoleng.2006.05.017)

Colas, F., V. Chanudet, M. Daufresne, L. Buchet, R. Vigouroux, A. Bonnet, F. Jacob, and J. M. Baudoin. 2020. Spatial and temporal variability of diffusive  $\text{CO}_2$  and  $\text{CH}_4$  fluxes from the Amazonian reservoir Petit-Saut (French Guiana) reveals the importance of allochthonous inputs for long-term C emissions. *Global Biogeochem. Cycl.* **34**: e2020GB006602. doi:[10.1029/2020GB006602](https://doi.org/10.1029/2020GB006602)

Deemer, B. R., and M. A. Holgerson. 2021. Drivers of methane flux differ between lakes and reservoirs, complicating global upscaling efforts. *J. Geophys. Res. Biogeosci.* **126**: 1–15. doi:[10.1029/2019JG005600](https://doi.org/10.1029/2019JG005600)

Delignette-Muller, L. M., C. Dutang, and J. Denis. 2015. fitdistrplus: An R package for fitting distributions. *J. Stat. Softw.* **64**: 1–34. doi:[10.18637/jss.v064.i04](https://doi.org/10.18637/jss.v064.i04)

Denfeld, B. A., H. M. Baulch, P. A. del Giorgio, S. E. Hampton, and J. Karlsson. 2018. A synthesis of carbon dioxide and methane dynamics during the ice-covered period of northern lakes. *Limnol. Oceanogr. Lett.* **3**: 117–131. doi:[10.1002/lo2.10079](https://doi.org/10.1002/lo2.10079)

Devlin, S. P., J. Saarenheimo, J. Syväranta, and R. I. Jones. 2015. Top consumer abundance influences lake methane efflux. *Nat. Commun.* **6**: 8787. doi:[10.1038/ncomms9787](https://doi.org/10.1038/ncomms9787)

Downing, J. A. 2009. Global limnology: Up-scaling aquatic services and processes to planet Earth. *Verhandlung. Int. Vereinigung Theor. Angew. Limnol.* **30**: 1149–1166. doi:[10.1080/03680770.2009.11923903](https://doi.org/10.1080/03680770.2009.11923903)

Downing, J. A. 2010. Emerging global role of small lakes and ponds: Little things mean a lot. *Limnetica* **29**: 9–24.

Finlay, K., R. J. Vogt, G. L. Simpson, and P. R. Leavitt. 2019. Seasonality of pCO<sub>2</sub> in a hard-water lake of the northern Great Plains: The legacy effects of climate and limnological conditions over 36 years. *Limnol. Oceanogr.* **64**: 118–129. doi:[10.1002/lno.11113](https://doi.org/10.1002/lno.11113)

Goodwin, K., N. Caraco, and J. Cole. 2008. Temporal dynamics of dissolved oxygen in a floating-leaved macrophyte bed. *Freshw. Biol.* **53**: 1632–1641. doi:[10.1111/j.1365-2427.2008.01983.x](https://doi.org/10.1111/j.1365-2427.2008.01983.x)

Grinham, A., S. Albert, N. Deering, M. Dunbabin, D. Bastviken, B. Sherman, C. Lovelock, and C. Evans. 2018. The importance of small artificial water bodies as sources of methane emissions in Queensland, Australia. *Hydrol. Earth Syst. Sci.* **22**: 5281–5298. doi:[10.5194/hess-2018-294](https://doi.org/10.5194/hess-2018-294)

Herb, W. R., and H. G. Stefan. 2004. Temperature stratification and mixing dynamics in a shallow lake with submersed macrophytes. *Lake Reserv. Manag.* **20**: 296–308. doi:[10.1080/07438140409354159](https://doi.org/10.1080/07438140409354159)

Hoffmann, S. S., J. F. Mcmanus, W. B. Curry, and L. S. Brown-leger. 2013. Persistent export of 231Pa from the deep central Arctic Ocean over the past 35,000 years. *Nature* **497**: 3–7. doi:[10.1038/nature12145](https://doi.org/10.1038/nature12145)

Hofmann, H. 2013. Spatiotemporal distribution patterns of dissolved methane in lakes: How accurate are the current estimations of the diffusive flux path? *Geophys. Res. Lett.* **40**: 2779–2784. doi:[10.1002/grl.50453](https://doi.org/10.1002/grl.50453)

Holgerson, M. A. 2015. Drivers of carbon dioxide and methane supersaturation in small, temporary ponds. *Biogeochemistry* **124**: 305–318. doi:[10.1007/s10533-015-0099-y](https://doi.org/10.1007/s10533-015-0099-y)

Holgerson, M. A., and P. A. Raymond. 2016. Large contribution to inland water CO<sub>2</sub> and CH<sub>4</sub> emissions from very small ponds. *Nat. Geosci.* **9**: 222–226. doi:[10.1038/ngeo2654](https://doi.org/10.1038/ngeo2654)

Holgerson, M. A., and others. 2022. Classifying mixing regimes in ponds and shallow lakes. *Water Resour. Res.* **58**: e2022WR032522. doi:[10.1029/2022WR032522](https://doi.org/10.1029/2022WR032522)

Huotari, J., A. Ojala, E. Peltomaa, J. Pumpanen, P. Hari, and T. Vesala. 2009. Temporal variations in surface water CO<sub>2</sub> concentration in a boreal humic lake based on high-frequency measurements. *Boreal Environ. Res.* **14**: 48–60.

Jensen, S. A., J. R. Webb, G. L. Simpson, H. M. Baulch, P. R. Leavitt, and K. Finlay. 2022. Seasonal variability of CO<sub>2</sub>, CH<sub>4</sub>, and N<sub>2</sub>O content and fluxes in small agricultural reservoirs of the northern Great Plains. *Front. Environ. Sci.* **10**: 895531. doi:[10.3389/fenvs.2022.895531](https://doi.org/10.3389/fenvs.2022.895531)

Kankaala, P., J. Huotari, T. Tulonen, and A. Ojala. 2013. Lake-size dependent physical forcing drives carbon dioxide and methane effluxes from lakes in a boreal landscape. *Limnol. Oceanogr.* **58**: 1915–1930. doi:[10.4319/lo.2013.58.6.1915](https://doi.org/10.4319/lo.2013.58.6.1915)

Kosten, S., M. Piñeiro, E. de Goede, J. de Klein, L. P. M. Lamers, and K. Ettwig. 2016. Fate of methane in aquatic systems dominated by free-floating plants. *Water Res.* **104**: 200–207. doi:[10.1016/j.watres.2016.07.054](https://doi.org/10.1016/j.watres.2016.07.054)

Kuznetsova, A., P. Brockhoff, and R. Christensen. 2017. lmerTest package: Tests in linear mixed effects models. *J. Stat. Softw.* **82**: 1–26. doi:[10.18637/jss.v082.i13](https://doi.org/10.18637/jss.v082.i13)

Laurion, I., W. F. Vincent, S. MacIntyre, L. Retamal, C. Dupont, P. Francus, and R. Pienitz. 2010. Variability in greenhouse gas emissions from permafrost thaw ponds. *Limnol. Oceanogr.* **55**: 115–133. doi:[10.4319/lo.2010.55.1.0115](https://doi.org/10.4319/lo.2010.55.1.0115)

Loken, L. C., J. Crawford, P. Schramm, P. Stadler, A. Desai, and E. Stanley. 2019. Large spatial and temporal variability of carbon dioxide and methane in a eutrophic lake. *J. Geophys. Res. Biogeosci.* **124**: 2248–2266. doi:[10.1029/2019JG005186](https://doi.org/10.1029/2019JG005186)

Lüdecke, D. 2021. sjstats: Statistical functions for regression models (Version 0.18.1). doi:[10.5281/zenodo.1284472](https://doi.org/10.5281/zenodo.1284472)

Marcé, R., B. Obrador, J. Morguí, J. L. Riera, P. López, and J. Armengol. 2015. Carbonate weathering as a driver of CO<sub>2</sub> supersaturation in lakes. *Nat. Geosci.* **8**: 107–111. doi:[10.1038/NGEO2341](https://doi.org/10.1038/NGEO2341)

Matveev, A., I. Laurion, B. N. Deshpande, N. Bhiry, and W. F. Vincent. 2016. High methane emissions from thermokarst lakes in subarctic peatlands. *Limnol. Oceanogr.* **61**: 150–164. doi:[10.1002/lno.10311](https://doi.org/10.1002/lno.10311)

McAuliffe, C. 1971. Gas chromatographic determination of solutes by multiple phase equilibrium. *Chem. Technol.* **1**: 46–51.

Messager, M. L., B. Lehner, G. Grill, I. Nedeva, and O. Schmitt. 2016. Estimating the volume and age of water stored in global lakes using a geo-statistical approach. *Nat. Commun.* **7**: 1–11. doi:[10.1038/ncomms13603](https://doi.org/10.1038/ncomms13603)

Natchimuthu, S., I. Sundgren, M. Gålfalk, L. Klemedtsson, and D. Bastviken. 2017. Spatiotemporal variability of lake pCO<sub>2</sub> and CO<sub>2</sub> fluxes in a hemiboreal catchment. *J. Geophys. Res. Biogeosci.* **122**: 30–49. doi:[10.1002/2016JG003449](https://doi.org/10.1002/2016JG003449)

Ollivier, Q. R., D. T. Maher, C. Pitfield, and P. I. Macreadie. 2019. Punching above their weight: Large release of greenhouse gases from small agricultural dams. *Glob. Chang. Biol.* **25**: 721–732. doi:[10.1111/gcb.14477](https://doi.org/10.1111/gcb.14477)

Pacheco, F. S., M. C. S. Soares, A. T. Assireu, M. P. Curtarelli, G. Abril, J. L. Stech, P. C. Alvalá, and J. P. Ometto. 2015. The effects of river inflow and retention time on the spatial heterogeneity of chlorophyll and water-air CO<sub>2</sub> fluxes in a tropical hydropower reservoir. *Biogeosciences* **12**: 147–162. doi:[10.5194/bg-12-147-2015](https://doi.org/10.5194/bg-12-147-2015)

Paranaíba, J. R., N. Barros, R. Mendonça, A. Linkhorst, A. Isidorova, F. Roland, R. M. Almeida, and S. Sobek. 2018. Spatially resolved measurements of CO<sub>2</sub> and CH<sub>4</sub> concentration and gas-exchange velocity highly influence carbon-emission estimates of reservoirs. *Environ. Sci. Technol.* **52**: 607–615. doi:[10.1021/acs.est.7b05138](https://doi.org/10.1021/acs.est.7b05138)

Paranaíba, J. R., N. Barros, R. M. Almeida, A. Linkhorst, R. Mendonça, R. do Vale, F. Roland, and S. Sobek. 2021. Hotspots of diffusive CO<sub>2</sub> and CH<sub>4</sub> emission from tropical

reservoirs shift through time. *J. Geophys. Res. Biogeo.* **126**: 1–19. doi:[10.1029/2020JG006014](https://doi.org/10.1029/2020JG006014)

Peacock, M., J. Audet, S. Jordan, J. Smeds, and M. B. Wallin. 2019. Greenhouse gas emissions from urban ponds are driven by nutrient status and hydrology. *Ecosphere* **10**: e02643. doi:[10.1002/ecs2.2643](https://doi.org/10.1002/ecs2.2643)

Peacock, M., and others. 2021. Small artificial waterbodies are widespread and persistent emitters of methane and carbon dioxide. *Glob. Chang. Biol.* **1–15**: 5109–5123. doi:[10.1111/gcb.15762](https://doi.org/10.1111/gcb.15762)

Podgrajsek, E., E. Sahlee, and A. Rutgersson. 2014. Diurnal cycle of lake methane flux. *J. Geophys. Res. Biogeo.* **119**: 2292–2311. doi:[10.1002/2013JG002327](https://doi.org/10.1002/2013JG002327)

Podgrajsek, E., E. Sahlee, and A. Rutgersson. 2015. Diel cycle of lake-air CO<sub>2</sub> flux from a shallow lake and the impact of waterside convection on the transfer velocity. *J. Geophys. Res. Biogeo.* **120**: 29–38. doi:[10.1002/2014JG002781](https://doi.org/10.1002/2014JG002781)

Praetzel, L. S. E., M. Schmiedeskamp, and K. H. Knorr. 2021. Temperature and sediment properties drive spatiotemporal variability of methane ebullition in a small and shallow temperate lake. *Limnol. Oceanogr.* **66**: 2598–2610. doi:[10.1002/lno.11775](https://doi.org/10.1002/lno.11775)

R Core Team. 2014. R: A language and environment for statistical computing. R Foundation for Statistical Computing.

Rabaey, J., and J. Cotner. 2022. Pond greenhouse gas emissions controlled by duckweed coverage. *Front. Environ. Sci.* **10**: 889289. doi:[10.3389/fenvs.2022.889289](https://doi.org/10.3389/fenvs.2022.889289)

Raymond, P. A., and others. 2013. Global carbon dioxide emissions from inland waters. *Nature* **503**: 355–359. doi:[10.1038/nature12760](https://doi.org/10.1038/nature12760)

Richardson, D. C., and others. 2022. A functional definition to distinguish ponds from lakes and wetlands. *Sci. Rep.* **12**: 10472. doi:[10.1038/s41598-022-14569-0](https://doi.org/10.1038/s41598-022-14569-0)

Rosentreter, J. A., and others. 2021a. Half of global methane emissions come from highly variable aquatic ecosystem sources. *Nat. Geosci.* **14**: 225–230. doi:[10.1038/s41561-021-00715-2](https://doi.org/10.1038/s41561-021-00715-2)

Rosentreter, J. A., A. V. Borges, B. R. Deemer, M. A. Holgerson, S. Liu, and C. Song. 2021b. Aquatic methane flux database. figshare Dataset.

Rudberg, D., and others. 2021. Diel variability of CO<sub>2</sub> emissions from northern lakes. *J. Geophys. Res. Biogeosci.* **126**: e2021JG006246. doi:[10.1029/2021jg006246](https://doi.org/10.1029/2021jg006246)

Scheffer, M. 2004. The story of some shallow lakes, p. 1–19. *In* *Ecology of shallow lakes*. Springer.

Schilder, J., D. Bastviken, M. Van Hardenbroek, P. Kankaala, P. Rinta, T. Stötter, and O. Heiri. 2013. Spatial heterogeneity and lake morphology affect diffusive greenhouse gas emission estimates of lakes. *Geophys. Res. Lett.* **40**: 5752–5756. doi:[10.1002/2013GL057669](https://doi.org/10.1002/2013GL057669)

Schindler, D. E., S. R. Carpenter, J. J. Cole, J. F. Kitchell, and M. L. Pace. 1997. Influence of food web structure on carbon exchange between lakes and the atmosphere. *Science* **277**: 248–251. doi:[10.1126/science.277.5323.248](https://doi.org/10.1126/science.277.5323.248)

Schmiedeskamp, M., L. S. E. Praetzel, D. Bastviken, and K. H. Knorr. 2021. Whole-lake methane emissions from two temperate shallow lakes with fluctuating water levels: Relevance of spatiotemporal patterns. *Limnol. Oceanogr.* **66**: 2455–2469. doi:[10.1002/lno.11764](https://doi.org/10.1002/lno.11764)

Sieczko, A. K., N. Thanh Duc, J. Schenk, G. Pajala, D. Rudberg, H. O. Sawakuchi, and D. Bastviken. 2020. Diel variability of methane emissions from lakes. *Proc. Natl. Acad. Sci. U.S.A.* **117**: 21488–21494. doi:[10.1073/pnas.2006024117](https://doi.org/10.1073/pnas.2006024117)

Torgersen, T., and B. Branco. 2008. Carbon and oxygen fluxes from a small pond to the atmosphere: Temporal variability and the CO<sub>2</sub>/O<sub>2</sub> imbalance. *Water Resour. Res.* **44**: 1–14. doi:[10.1029/2006WR005634](https://doi.org/10.1029/2006WR005634)

Tranvik, L. J., and others. 2009. Lakes and reservoirs as regulators of carbon cycling and climate. *Limnol. Oceanogr.* **54**: 2298–2314. doi:[10.4319/lo.2009.54.6\\_part\\_2.2298](https://doi.org/10.4319/lo.2009.54.6_part_2.2298)

Vachon, D., and Y. T. Prairie. 2013. The ecosystem size and shape dependence of gas transfer velocity versus wind speed relationships in lakes. *Can. J. Fish. Aquat. Sci.* **70**: 1757–1764. doi:[10.1139/cjfas-2013-0241](https://doi.org/10.1139/cjfas-2013-0241)

Waldo, S., J. J. Beaulieu, W. Barnett, D. A. Balz, M. J. Vanni, T. Williamson, and J. T. Walker. 2021. Temporal trends in methane emissions from a small eutrophic reservoir: The key role of a spring burst. *Biogeosciences* **18**: 5291–5311. doi:[10.5194/bg-18-5291-2021](https://doi.org/10.5194/bg-18-5291-2021)

Weiss, R. F. 1974. Carbon dioxide in water and seawater: The solubility of a non-ideal gas. *Mar. Chem.* **2**: 203–215.

Wiesenburg, D. A., and N. L. Guinasso. 1979. Equilibrium solubilities of methane, carbon monoxide, and hydrogen in water and sea water. *J. Chem. Eng. Data* **24**: 356–360. doi:[10.1021/je60083a006](https://doi.org/10.1021/je60083a006)

Wiik, E., H. Haig, N. Hayes, K. Finlay, G. Simpspon, R. Vogt, and P. Leavitt. 2018. Generalized additive models of climatic and metabolic controls of subannual variation in pCO<sub>2</sub> in productive hardwater lakes. *J. Geophys. Res. Biogeo.* **123**: 1940–1959. doi:[10.1029/2018JG004506](https://doi.org/10.1029/2018JG004506)

Wik, M., B. F. Thornton, D. Bastviken, J. Uhlbäck, and P. M. Crill. 2016. Biased sampling of methane release from northern lakes: A problem for extrapolation. *Geophys. Res. Lett.* **43**: 1256–1262. doi:[10.1002/2015GL066501](https://doi.org/10.1002/2015GL066501). Received

#### Acknowledgments

The authors thank Kathryn Hoffman, Margot Groskreutz, Kari Dawes, Heather Wander, Sabrina Volponi, Brenna O'Brien, Mei Schultz, Paige Kowal, Jillian St. George, Eliane Demierre, and Beat Oertli for assistance with sample collection and processing. Jane Byron and Jessie Koehle facilitated site selection and access to sites in Rosemount and Eagan, Minnesota, respectively. Stephen Parry from the Cornell Statistical Consulting Unit provided helpful guidance on our statistical approach. Emily Moothart aided in making the map. Funding for this research was provided by several sources. M.A.H was supported by the St. Olaf College Collaborative Undergraduate Research and Inquiry program. M.R.A was supported as part of the BEYOND 2020 project (grant-aid agreement no. PBA/FS/16/02) by the Marine Institute and funded under the Marine Research Program by the Irish Government. D.C.R. received funding through the SUNY New Paltz Research and Creative Arts program and National Science Foundation award 1559769.

J.P.M. was funded by the European Union's Horizon 2020 Research and Innovation Program under the Marie Skłodowska-Curie grant agreement no. 722518 (MANTEL ITN) and by the European Union's Horizon 2020 research and innovation program within the framework of the project SMARTLAGOON, grant agreement number 101017861. K.M.C. through The National Ecological Observatory Network, a program sponsored by the National Science Foundation and operated under cooperative agreement by Battelle. This material is based in part upon work supported by the National Science Foundation through the NEON Program. M.P. and M.F. were funded by Formas grant 2020-00950 and Naturvårdsverket grant 802-0083-19. I.K. and J.B. were funded by the University of Latvia grant No. ZD2016/AZ107. S.B. was funded by the U.S. Geological Survey, Ecosystems Mission Area, Land Change Science Program. Any use of trade,

firm, or product names is for descriptive purposes only and does not imply endorsement by the U.S. Government.

### Conflict of Interest

The authors declare that they have no competing interests.

Submitted 04 April 2022

Revised 31 January 2023

Accepted 15 April 2023

Associate editor: John A. Downing